

# Quark-nova explosion inside a collapsar: application to Gamma Ray Bursts

Rachid Ouyed, Denis Leahy, Jan Staff, and Brian Niebergal

Department of Physics and Astronomy, University of Calgary, 2500 University Drive NW, Calgary, Alberta, T2N 1N4 Canada\*

Received ;date; accepted ;date;

**Abstract.** If a quark-nova occurs inside a collapsar, the interaction between the quark-nova ejecta (relativistic iron-rich chunks) and the collapsar envelope, leads to features indicative of those observed in Gamma Ray Bursts. The quark-nova ejecta collides with the stellar envelope creating an outward moving cap ( $\Gamma \sim 1-10$ ) above the polar funnel. Prompt gamma-ray burst emission from internal shocks in relativistic jets (following accretion onto the quark star) become visible after the cap becomes optically thin. Model features include: (i) precursor activity (optical, X-ray,  $\gamma$ -ray), (ii) prompt  $\gamma$ -ray emission, and (iii) afterglow emission. We discuss SN-less long duration GRBs, short hard GRBs (including association and non-association with star forming regions), dark GRBs, the energetic X-ray flares detected in Swift GRBs, and the near-simultaneous optical and  $\gamma$ -ray prompt emission observed in GRBs in the context of our model.

**Key words.** Collapsar – QuarkNova – Supernova – quark star – GRBs

## 1. INTRODUCTION

Recent observations following the launch of the *Swift* satellite challenge the traditional models of GRBs (e.g. Mészáros 2006; Zhang 2008). In particular the traditional afterglow modeling, which has been successful in many ways, appears to have serious limitations (e.g. Granot 2008 for a recent review). Here we show how appealing to a quark-nova occurring inside a collapsar can lead to phenomenology reminiscent of that seen by Swift. We start with a brief review of the Quark-Nova explosion.

A quark-nova (QN), (Ouyed, Dey, & Dey 2002; Keränen&Ouyed 2003; Keränen, Ouyed, & Jaikumar 2005) is the explosion driven by phase transition of the core of a neutron star (NS) to the quark matter phase (i.e neutron star core collapse) leading to the formation of a quark star (QS). The gravitational potential energy released (plus latent heat of phase transition) during this event is converted partly into internal energy and partly into outward propagating shock waves which impart kinetic energy to the material that forms the ejecta (i.e. the outermost layers of the neutron star crust). The ejection of the outer layers of the NS is driven by the thermal fireball generated as the star cools from its birth temperature down to  $\sim 7.7$  MeV (Vogt, Rapp, & Ouyed 2004; Ouyed, Rapp, & Vogt 2005). The fireball expands approximately adiabatically while pushing the overlaying crust, and cooling fairly rapidly. The energy needed to eject the crust is less than 1% of fireball energy.

The initial composition of the ejecta is representative of matter in the outer layers of the neutron star crust (with den-

sity below  $\sim 10^{11} \text{ g cm}^{-3}$ ), dominated by iron-group elements and neutron-rich large  $Z$  nuclei beyond iron (Baym, Pethick, & Sutherland 1971). As the ejecta expands, r-process takes effect leading to the formation of even heavier elements. As shown in Jaikumar et al. (2007), the QN is effective at turning at most 10% of the ejecta into elements above  $A \sim 130$  (Jaikumar et al. 2007). In previous work we explored the dynamical and thermal evolution of this ejecta (Ouyed&Leahy 2008; Leahy&Ouyed 2008a). As the ejecta moves outwards it expands and cools undergoing a liquid to solid transformation<sup>1</sup>. The relativistic expansion causes rapid breakup into small chunks because of the inability of causal communication laterally in the shell. Whether liquid or solid iron, inter-ionic forces (mediated by the electrons) provide the tension leading to breakup (which does not occur for a gas). The size of the clumps depends on whether the breakup occurs in the liquid or solid phase. In the solid/liquid phase the ejecta breaks up into  $\sim 10^7/10^3$  chunks with chunk mass of  $\sim 10^{19}/10^{23}$  gm. Table 1 in Ouyed&Leahy (2008) lists the properties of the clumps/chunks.

In this paper, we explore consequences of a quark nova occurring during the supernova explosion in a rotating massive star. Before the QN has occurred, one has the progenitor col-

<sup>1</sup> For ejecta birth temperature of the order of 10 MeV, the relativistic electrons are only mildly degenerate (see appendix in Ouyed&Leahy 2008). Thus additional heat deposition into the ejecta during the expansion (e.g. due to nuclear decays of r-processed elements) could lead to non-degeneracy leaving the ejecta in gaseous form. Here, we assume that the degeneracy is not lifted during the early ejecta expansion.

\* email:ouyed@phas.ucalgary.ca

lapse – much like in the collapsar picture except that in our case a QS is formed instead of a black hole (BH) (see Fig. 1). We note that for low angular momentum progenitors, the combination of a high NS core density at birth and, most likely, fall-back material would drive the proto-neutron star to a black hole. High angular momentum progenitors (collapsars), will delay the formation of a black hole for three main reasons: (a) the progenitor’s core tends to shed more mass and angular momentum as it shrinks reducing central core mass and fall-back; (b) high spin keeps the core density of the resulting neutron star from crossing the black hole formation limit; (c) high angular momentum in the material around the core reduces the accretion rate onto the central object. The subsequent accretion onto the quark star explains the prompt emission in our model (Ouyed et al. 2005). The conversion from NS to QS depends on the NS central density at birth. As shown by Staff et al. (2006), spin-down leads to increase of core density and subsequent conversion. Thus progenitor’s angular momentum does not mean the conversion to QS is unlikely, it only affects the delay between the SN and QN. In summary, collapsars seem to provide favorable conditions for the QN to occur inside them. Furthermore, the high angular momentum in the envelope leads to funnel formation which allows the QS jet to escape the envelope and the GRB to be visible.

The paper is structured as follows: In section 2 we investigate the ejecta interaction with the stellar envelope for the two cases of thin and thick envelope. In section 3 we apply our model to GRBs and explain how the interaction of the chunks with the stellar envelope can lead to precursor, prompt and afterglow emissions reminiscent of those observed in GRBs. A discussion is given in section 4 before concluding in section 5.

## 2. Ejecta’s Interaction with stellar envelope

Wolf-Rayet stars can have extended envelopes, the profile of which depends on evolution and metallicity. The evolutionary effects generally result in WN (nitrogen burning) stars evolving into WC (carbon burning) stars with much smaller masses and radii due to mass-loss (e.g. Meynet & Maeder 2003; Heger et al. 2003). What is of interest here is the structure of the envelope at the time of stellar collapse, which is not yet fully understood. For simplicity, we take the stellar structure of a Helium Wolf-Rayet star (Petrovic et al. 2006) to be representative of the progenitor and consider the low and high-metallicity cases (see their Figure 2). The main difference is that the high metallicity star has an extended envelope with density  $\sim (10^{-10}-10^{-9}) \text{ g cm}^{-3}$  and a density inversion near the surface ( $\sim 3R_\odot$  for a  $24M_\odot$  star). In the low metallicity case, the star envelope cuts off sharply at  $\sim 1.5R_\odot$ .

When the broken pieces of ejecta impact this stellar envelope they undergo a shock and become heated to a temperature

$$T_c \sim \xi_s \Gamma_i \frac{A}{1+Z} m_H c^2, \quad (1)$$

where  $\Gamma_i$  is the Lorentz factor of the ejecta and  $m_H$  the proton mass. Equation above shows that the chunk temperature is insensitive to the presence of heavier elements since  $A/(1+Z)$  does not vary much. Hereafter, and for simplicity, we assume

an iron-dominated ejecta (i.e.  $A=56$  and  $Z=26$ ). Here, the shock efficiency was roughly estimated to be  $\xi_s \sim (\rho_{\text{env.}}/\rho_{\text{Fe}})^2$ , where  $\rho_{\text{env.}}$  is the envelope density at the shock radius. Noting that non-degenerate iron will vaporize if heated to  $\geq 0.3 \text{ eV}$  (see CRC tables 2005 for vaporization temperature of iron at normal density), we then define a critical envelope density  $\rho_{\text{env.,c}} \sim 10^{-5} \text{ g cm}^{-3}$  above which the chunks will be vaporized and lose considerable momentum.

One might argue that normal core collapse supernovae accompanied by quark novae, should be more energetic than the canonical  $\sim 10^{51}$  ergs observed. However, this depends on the delay between the SN and the QN. If the delay between the QN and SN is long enough, the chunks will not re-energize the SN. The mean density in the envelope ( $\bar{\rho}_{\text{env.}} \propto M_{\text{env.}}/R_{\text{env.}}^3$  in the simplest of cases) depends on (i) the progenitor’s pre-collapse profile (which depends on evolution and metallicity) and (ii) on the delay between the QN and SN. The longer the delay, the smaller the envelope density when the chunks hit it. For a typical  $5M_\odot$  envelope we find that  $\bar{\rho}_{\text{env.}} \sim \rho_{\text{env.,c}}$  is reached when the envelope is at  $R_{\text{env.}} \sim 10^{13} \text{ cm}$ . In other words, for cases where the delay between the SN and QN exceeds a few days (for SN ejecta velocity  $\sim 1000 \text{ km s}^{-1}$ ), the QN ejecta will encounter a thin envelope yielding weak interaction. For more massive envelopes, delays of the order of weeks are required for the density to drop below critical; shorter delays lead to complete dissipation of the chunks energizing the preceding supernova remnant. As shown in Leahy&Ouyed (2008b), this can account for superluminous supernovae such as SN 2006gy. The density of the stellar envelope along the rotation axis is also affected by rotation. For a rotating progenitor the collapse proceeds fastest along the polar axis leaving a low density path called the funnel (Woosley&Bloom 2006 and references therein), with opening half angle  $\theta_f$ . If the QN ejecta propagated into this funnel, then it would encounter negligible resistance (i.e. thin envelope case), while in other directions the QN ejecta would interact with the higher density SN ejecta (see Fig. 1). In these equatorial regions most of the QN energy is lost to energizing the SN ejecta and only a fraction ( $\sim 2.5 \times 10^{49} \text{ erg } \eta_{0.1} \theta_{f,0.1}^2 E_{\text{QN},53}$ ) is directed into the funnel. The bulk of the ejecta energy not entering the funnel,  $\sim 10^{52} \text{ erg } \eta_{0.1} E_{\text{QN},53}$ , goes into re-energizing the SN ejecta and can result in a hypernova (see discussion in § 4.4).

### 2.1. Thick envelope

If the envelope density is higher than  $\rho_{\text{env.,c}}$ , the chunks will be vaporized upon impact leading to runaway dissipation and total merging of the ejecta with the envelope. A significant fraction,  $m_{\text{env.}}/(m_{\text{env.}} + m_{\text{ejecta}})$ , of the kinetic energy of the QN ejecta goes into heating the envelope. In this case, the thermal energy of the combined ejecta and envelope (hereafter referred to as the cap) is

$$E_{\text{th.}} = \frac{m_{\text{env.}}}{m_{\text{env.}} + m_{\text{ejecta}}} \frac{\pi \theta_f^2}{4\pi} \Gamma_i m_{\text{ejecta}} c^2, \quad (2)$$

where the resulting thermal energy per nucleus is,

$$kT_{\text{nuc}} \sim \frac{m_{\text{ejecta}} m_{\text{env.}}}{(m_{\text{ejecta}} + m_{\text{env.}})^2} \Gamma_i \mu m_H c^2, \quad (3)$$

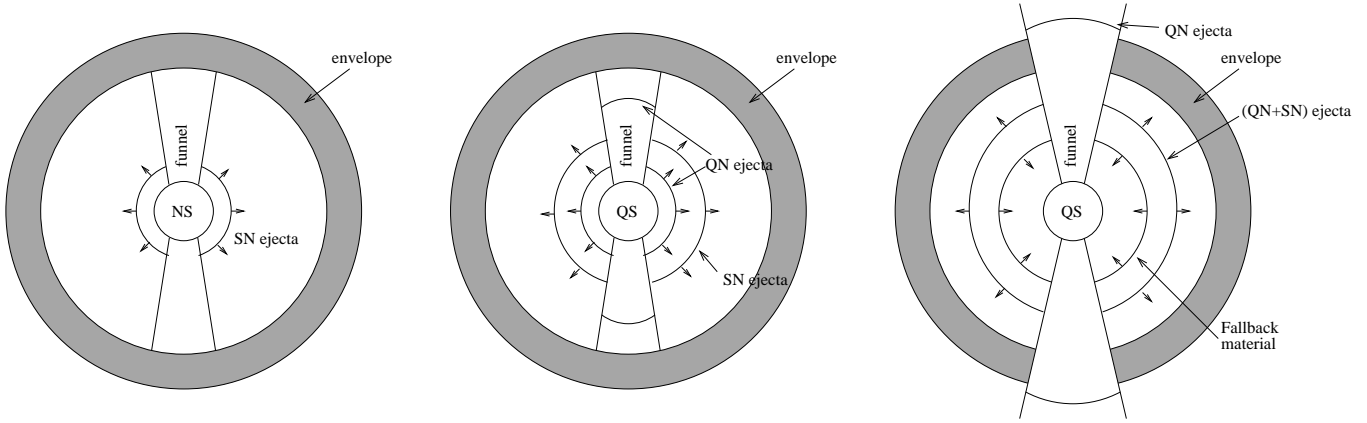


**Fig. 1.** Outline of the initial phases for GRBs from Quark-Novae (QN). *Stage 1:* A newly formed neutron star with expanding ejecta and SN shock wave, as well as the stationary WR stellar envelope is also shown. Angular momentum of the progenitor results in low density polar funnels. *Stage 2:* An explosive neutron star to quark star conversion (i.e. Quark-Nova) occurs producing the QN ejecta. The QN ejecta can then propagate freely through the funnel, while in other directions it will overtake the SN ejecta. *Stage 3:* The QN ejecta along the funnel interacts with the WR stellar envelope, while the collision of the SN and QN ejecta lead to an energized outgoing ejecta (suggestive of a hypernova).

with  $\mu$  the mean mass per nucleus. The maximum nucleus temperature,  $T_{\text{nuc,max}} \sim 2.4 \text{ GeV } \Gamma_{i,10}\mu$ , occurs when the envelope and ejecta masses are equal;  $\Gamma_{i,10}$  is the ejecta's initial Lorentz factor in units of 10. Note that,  $\mu \sim 1$  whenever  $T_{\text{env}}$  exceeds 1 MeV due to nuclear dissociation. Thermalization with  $(e^+e^-)$  pair creation places an upper limit on the electron temperature of  $\sim 1 \text{ MeV}$ . Subsequent energy transfer from nuclei to electrons contributes to further pair creation as the nuclei cool to 1 MeV. If  $kT_{\text{nuc}} > 1 \text{ MeV}$ , then most of the ejecta's kinetic energy ends up as  $(e^+e^-)$  pairs. The end result would then be a cap rich in pairs.

Momentum conservation arguments in this case show that the cap slows quickly, reaching a final speed ( $v_f$ ) of,

$$\beta_f \Gamma_f = \frac{\sqrt{\Gamma_i^2 - 1}}{1 + \frac{m_{\text{env}}}{m_{\text{ejecta}}}}, \quad (4)$$

where  $\beta_f = v_f/c$ . We note that if the envelope mass is less than  $m_{\text{env,R}} \sim 10^{-3} M_{\odot} \Gamma_{i,10} m_{\text{ejecta}}^{-4}$ , then the mixed ejecta is moving radially outwards at relativistic speeds ( $\beta_f \Gamma_f > 1$  or  $\beta_f > 1/\sqrt{2}$ ; see Fig. 2). Thus  $m_{\text{env,R}}$  separates two regimes within the thick envelope case which is of relevance when applying our model to GRBs.

## 2.2. Thin envelope

If the stellar envelope density following the collapse is below the critical density,  $\rho_{\text{env,c}}$ , the chunks will not be vaporized nor do they expand significantly, rather they pass through the envelope effectively puncturing it. During this interaction the temperature of a piece of broken ejecta,  $T_c$ , is determined by shock heating (eq. 1), and will not exceed the eV range; thus any emission would be in the optical band (see §3.1.1). As discussed above, high metallicity stars can have extended thin envelopes. However, inhomogeneities and asphericity in the thick envelope case could lead to low-density regions where the chunks can survive destruction.

## 3. Application to GRBs

The advent of the *Swift* mission has enabled a much more intensive sampling of GRB light curves, particularly during its early phases but also extending out to late times. These data allow for a more stringent comparison with the standard blast wave model. In addition to the suggested extended engine activity, the observed X-ray flares (e.g. Nousek et al. 2006) appear to be a distinct emission component, which suggests a sporadic late time activity of the central source. Another interesting finding by *Swift* is that the early optical emission, which has been attributed in some cases before *Swift* to the reverse shock, is typically dimmer than expected. The chromatic breaks in the afterglow lightcurves is puzzling as it suggests that the X-ray and optical emission may arise in separate physical components, which would then naturally account for their seemingly decoupled lightcurves. There are other features that seem difficult to explain within the framework of the standard engine and afterglow (we refer the interested reader to Granot 2008 for more on this).

Here we show how appealing to a quark-nova following the SN can help alleviate at least some of the issues mentioned above. The interaction of the QN ejecta with the stellar envelope yields precursors and postcursors in the optical and X-ray range as shown next.

### 3.1. Precursors

#### 3.1.1. Thin envelope (optical precursor)

In our model, the mechanism for production of an optical flash is the heating of the chunks of the QN ejecta in the thin envelope case. In this case, emission is directly related to shock efficiency with emitted energy,

$$E_{\text{p,O}} \sim (\xi_s \Gamma_i \mu_e m_{\text{ejecta}} c^2) \times \Gamma_i^2 \quad (5) \\ \sim 10^{41} \text{ ergs } \xi_{s,c} \Gamma_{i,10}^3 m_{\text{ejecta}}^{-4},$$

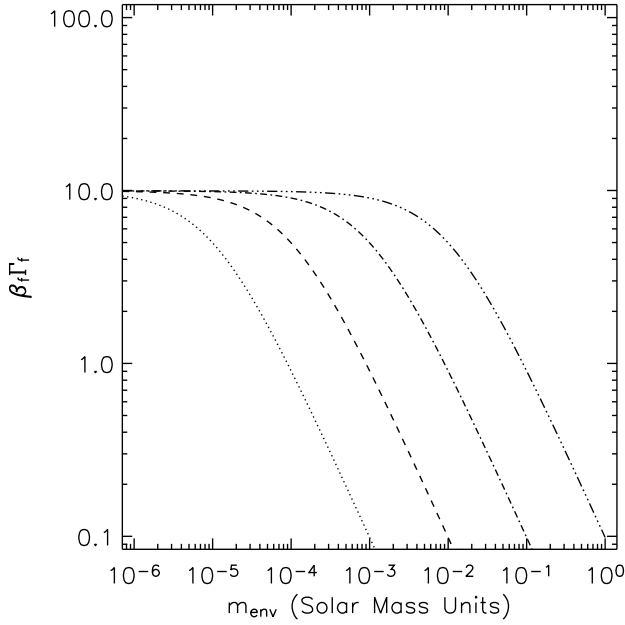


**Fig. 2.** Final velocity ( $\beta_f \Gamma_f$ ; Eq. 4) of the combined mass of the envelope plus ejecta following collision. The four curves are for ejecta masses ranging from  $10^{-5} M_\odot$  to  $10^{-2} M_\odot$ , left to right (all with a QN ejecta with  $\Gamma_i = 10$ ). The transition from relativistic to non-relativistic bulk motion occurs at  $\beta_f \Gamma_f = 1$ .

where  $\xi_{s,c} = (\rho_{\text{env},c}/\rho_{\text{Fe}})^2$  and  $\mu_e \sim 2$  is the mean weight per electron. The precursor optical emission we expect to be thermal-like despite such a relativistic beaming; equation above takes into account beaming correction ( $\Gamma_i^2 \sim 100$ ).

The precursor time is governed by 3 timescales:

- (a) time to traverse the envelope, if the envelope is optically thin to the radiation emitted at temperature  $T_c$ ;
- (b) geometrical time delay ( $\theta_f R_{\text{env}}/c$ );
- (c) cooling time of the chunk:  $t_{\text{cool}} \sim (3/2)kT_c N_{\text{Fe}}/L$  with  $L = A_c \sigma T_c^4$ ; the chunk's area is  $A_c \sim 6 \times 10^{11} \text{ cm}^2$ .

The number of particles in the chunk is  $N_{\text{Fe}} \sim m_c/(\mu m_p) \sim 2 \times 10^{44}$  with  $\mu \sim 28$  (if we take one ion and one free electron in the metal per Fe nucleus). Then  $t_{\text{cool}} \sim 0.8 \text{ s} \times T_{\text{keV}}^{-3}$  and depends strongly on the temperature that the chunks are heated to. If optical (eV) then (c) is longer than (a) so the longer of (b) and (c) would give the observed precursor duration. If the chunks are heated to keV temperatures, (c) is so short that unless the chunk is continuously heated by interaction with the envelope, the longer of (a) or (b) would give observed precursor duration. The observed cooling time is shorter by a factor of  $1/(2\Gamma_c^2)$  due to relativistic motion of the chunk toward the observer. We note that for liquid clumps  $N_{\text{Fe}}$  and the area  $A_c$  are both larger somewhat lengthening  $t_{\text{cool}}$ . But  $t_{\text{cool}}$  is still dominated by the value of  $T_{\text{keV}}$  leading to the same conclusions.

Near-simultaneous optical and  $\gamma$ -ray emission has been observed in a few cases (e.g. Zou, Piran, & Sari 2008). This has

led to open debates on the association or non-association between the two emissions (e.g. Kumar&Panaiteanu 2008). This is further discuss in §4.5. Let us simply mention that in our model, any observation of optical precursor, means that the envelope density must be close to  $\rho_{\text{env},c}$  with chunks heated to 0.3 eV (i.e.  $T_{\text{observed}} = \Gamma_i \times 0.3 \text{ eV} \sim 3 \text{ eV}$ ). In those sources, the observed optical precursor could yield crucial information about the delay between the SN and QN.

### 3.1.2. Thin envelope with density inversion (optical and X-ray precursors)

After the chunks have freely propagated outside of the main envelope they can interact with a higher density shell further out at a radius of  $r_{\text{inv}}$  (i.e. the density inversion in the envelope at a few times  $10^{11} \text{ cm}$ ; e.g. figure 2 in Petrovic et al. 2006). In order for the chunks to dissipate their energy, the density of the outer shell must exceed  $\rho_{\text{env},c} \sim 10^{-5} \text{ g cm}^{-3}$  (from § 2). Once the chunks collide with matter possessing this critical density they spread, resulting in their density decreasing, initiating a runaway dissipation process, ionization and heating. The emission from the shocked material is optically thin so the observer sees radiation at the shock temperature  $T_c$  as given in equation (1). For example, if the density at the inversion is  $\sim 100 \rho_{\text{env},c}$ , then the X-ray emission will peak at  $\sim 3 \text{ keV}$ .

Since the mass at of the envelope at the inversion radius is much less than the ejecta mass, the shock propagates at  $\sim \Gamma_i$ . Since  $1/\Gamma_i \geq \theta_f$ , an observer would see the emission from all of the chunks, and so the overall precursor pulse would be due to the sequential viewing of different individual pulses from each chunk along the curved surface. The precursor duration is then due to a geometrical delay,

$$t_{\text{prec}} \sim \frac{\theta_f r_{\text{inv}}}{c} \sim 3 \text{ s } \theta_{f,0.1} r_{\text{inv},12} . \quad (6)$$

### 3.1.3. Thick envelope case ( $\gamma$ -ray Precursor)

If significant portions of the stellar envelope are above the critical density, then one would expect the kinetic energy of the chunks to be deposited in a thin dissipation zone at the base of the envelope. This will effectively spread the ejecta, forming a piston with a strong shock ahead of it. This piston should remain relativistic until it has swept up approximately  $\Gamma_i m_{\text{ejecta}}$  of envelope mass, at which point it slows, reaching a final velocity given by equation (4). Although the shock heats up and dissociate the nuclei, however, as noted above, the actual temperature<sup>2</sup> will be limited to  $\sim 1 \text{ MeV}$  due to thermal ( $e^+e^-$ ) pair creation.

<sup>2</sup> The details of the shock heating of the envelope and its subsequent cooling are complex. Using blackbody cooling as an upper limit leads to an extremely rapid cooling time (mainly due to the large emitting area) of  $t_{\text{env,cool}} \sim 10^{-12} \text{ s } m_{\text{env},-4}/T_{\text{env},1}^3$ , where the envelope temperature is in units of 1 MeV. We note that the actual cooling time is defined by the shock propagation time through the optically thin outer parts of the envelope ( $\sim 10^5 \text{ cm}$ ), which yields timescales  $\leq 10^{-4} \text{ s}$ .



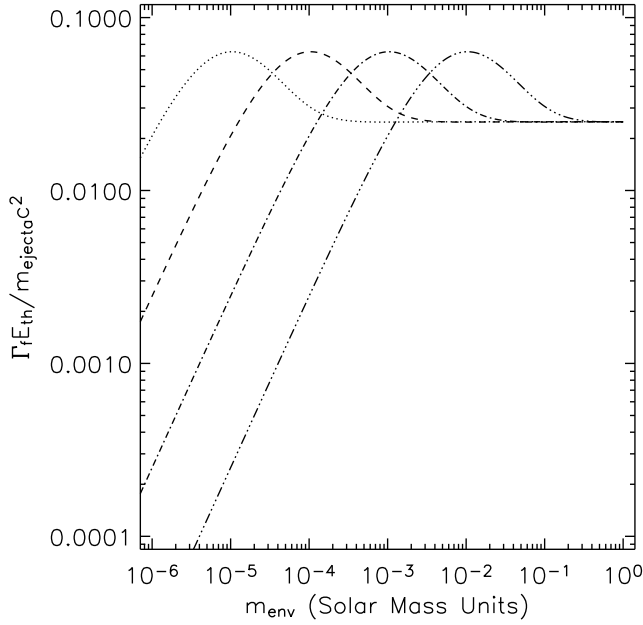


**Fig. 3.** Estimated fluence of the precursor in the thick envelope case (from Eq. 2). The four curves are for ejecta masses from  $10^{-5} M_{\odot}$  to  $10^{-2} M_{\odot}$  from left to right (all with a QN ejecta with  $\Gamma_i = 10$ ). The peak fluence occurs at  $m_{\text{ejecta}} = 2m_{\text{env}}$  with a value of about 6% of  $m_{\text{ejecta}} c^2$ .

The precursor consists of a short burst of radiation when the shock reaches the outer edge of the envelope. The precursor would have a typical temperature of a pair plasma,  $T_{\text{prec.}} \sim 500$  keV with a duration also defined by geometrical delays,

$$t_{\text{prec.}} \sim \frac{\theta_f r_{\text{env.}}}{c} \sim 0.3 \text{ s } \theta_{f,0.1} r_{\text{env.,11}}. \quad (7)$$

The precursor brightness in the thick envelope case depends on the final speed of the combined ejecta: (i) if it is relativistic ( $m_{\text{env.}} < m_{\text{env.,R}}$ ) the usual blueshift and beaming applies yielding higher brightness ( $\propto \Gamma^2$ ); (ii) if it is not relativistic we expect the precursor to be dimmer and harder to detect.

We approximate the precursor fluence by assuming that all of the thermal energy is radiated. In the non-relativistic case and for  $m_{\text{env,c.}} < m_{\text{env,R}} < m_{\text{env}}$

$$E_p \sim 2.5 \times 10^{49} \text{ ergs } \eta_{0.1} \theta_{f,0.1}^2 E_{\text{QN},53}, \quad (8)$$

while the resulting fluence in the relativistic case (i.e.  $m_{\text{env,c.}} < m_{\text{env}} < m_{\text{env,R}}$ ) is written as  $\Gamma_f E_{\text{th.}}$  and is shown in Figure (3). It peaks at  $(2\Gamma_i^2/9)(\theta_f^2/4)m_{\text{ejecta}} c^2$ , or,

$$E_{p,\text{max}} \sim 2.5 \times 10^{50} \text{ erg } \frac{\theta_{f,0.1}^2 \eta_{0.1}^2 E_{\text{QN},53}^2}{m_{\text{ejecta},-4}}. \quad (9)$$

Note that when  $m_{\text{ejecta}}/m_{\text{env.}} < 10^{-5}$ , the thermal energy per nucleus is in the keV range leading to an X-ray precursor instead of a  $\gamma$ -ray precursor.

### 3.2. Prompt GRB emission

As shown in Figure 4, the phase following the precursor phase consists of the quark star accreting the disk material. As shown in Ouyed et al. (2005) whenever the quark star is heated above  $T_a \sim 7.7$  MeV it will release a burst of photons with energy  $\sim 3T_a$  which can momentarily impede accretion, until the burst has faded at which point another accretion episode ensues leading to another burst. In its simplest form, this episodic process (Ouyed et al. 2005) can be responsible for creating intermittent fireballs (loaded shells with Lorentz factor in the hundreds) eventually leading to internal shocks as described by Kobayashi et al. (1997). Compared to any other jet launching mechanism (e.g. from a black hole), the QS is able to emit far more energy for a given amount of accreted material (Vogt et al. 2004; Ouyed et al. 2005). Part of the effectiveness of our model can be attributed to the high efficiency in which the QS converts accreted matter to radiation.

The column density of the cap is

$$N_{\text{cap}} \sim \frac{m_{\text{cap}}/4\pi}{56m_{\text{H}}r_{\text{em}}^2} \sim 2 \times 10^{27} \text{ cm}^{-2} \frac{m_{\text{cap},-4}}{r_{\text{em},12}^2}, \quad (10)$$

with a corresponding optical depth

$$\tau_{\text{cap}} \simeq N_{\text{cap}} \sigma_T \sim 1325 \frac{m_{\text{cap},-4}}{r_{\text{em},12}^2}, \quad (11)$$

where  $\sigma_T$  is the Thompson cross-section. This implies that the cap is initially Compton optically thick to the photons from the internal shocks occurring underneath. Thus the prompt GRB phase can only be observed as optically thin once the cap is somehow destroyed or pushed to a higher radius by the QS shells.

#### 3.2.1. Cap acceleration and removal

In the thin envelope case, the first few shells from the QS accretion phase could easily remove the opaque envelope material, making subsequent bursts detectable by the observer. Alternatively, in the case of a thick envelope, the cap will be bombarded by many QS shells before it starts accelerating. In general the number of collisions with the QS shells needed to dissipate or remove the cap to distances large enough to become transparent to radiation is  $\sim \Gamma_f m_{\text{cap}}/\Gamma_{\text{shell}} m_{\text{shell}}$ . That is, about 100 collisions using our fiducial values. Equation (11) above indicates that  $\tau_{\text{cap}} \sim 1$  at a radius  $\sim 3 \times 10^{13} \text{ cm } m_{\text{cap},-4}$  which occurs at time  $\sim 1000 \text{ s } m_{\text{cap},-4}$

#### 3.2.2. Cap temperature and spectrum

An approximate equilibrium temperature for the cap can be found from the relation,  $\epsilon_r R_{\text{QS}}^2 T_{\text{QS}}^4 \sim r_{\text{em}}^2 T_{\text{eq,cap}}^4$ , which yields

$$T_{\text{eq,cap}} \sim 100 \text{ keV } T_{\text{QS},10} \epsilon_{r,0.1}^{1/4} \left( \frac{R_{\text{QS},10}}{r_{\text{em},12}} \right)^{1/2}, \quad (12)$$

where  $T_{\text{QS},10}$  and  $R_{\text{QS},10}$  are the QS temperature and radius in units of 10 MeV and 10 km, respectively;  $\epsilon_{r,0.1}$  is the radiative efficiency of the internal shocks which we take to be  $\sim 10\%$

## QN-GRB with SN

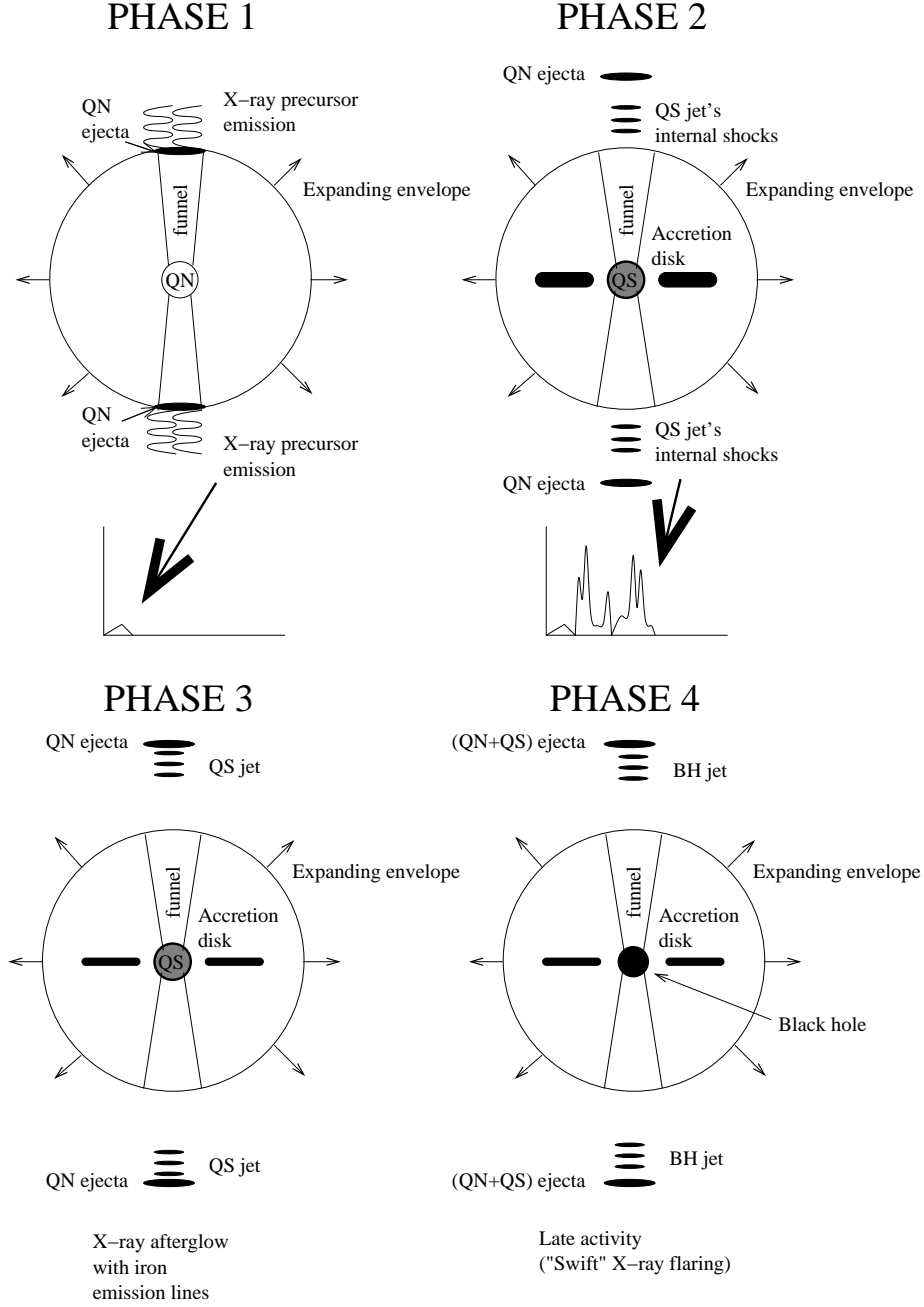


**Fig. 4.** Shown in this figure are three sequential phases and a fourth possible phase in our model for the case of a SN (i.e. expanding envelope). Phase 1 consists of the interaction between the QN ejecta and the envelope leading to an X-ray precursor (see §2.2). An accretion disk forms around the QS leading to Phase 2 where a jet is launched, providing the prompt GRB emission (see §3.2). Phase 3 shows the late stages of the QS jet interacting with the QN ejecta leading to an X-ray afterglow. However, if accretion is sufficiently large the QS may turn into a BH (phase 4 above), causing launch of a second jet extending the prompt GRB phase reminiscent of late time activity observed by Swift (see Staff et al. 2006b)

(Kobayashi et al. 1997). This equilibrium temperature is actually the peak temperature because the QS heating is episodic (see Ouyed et al. 2005) and the temperature is only lower in between episodes. This quasi-continuous supply of photons by the QS will keep the fireball spectra close to thermal during its

evolution. The spectra should thus consist of a blackbody in the early phase which would eventually evolve into an optical thin emission. Interestingly, it has been suggested in the literature that a hybrid model with a thermal and non-thermal component can explain all type of spectral evolution and shapes of the ob-

## QN-GRB without SN

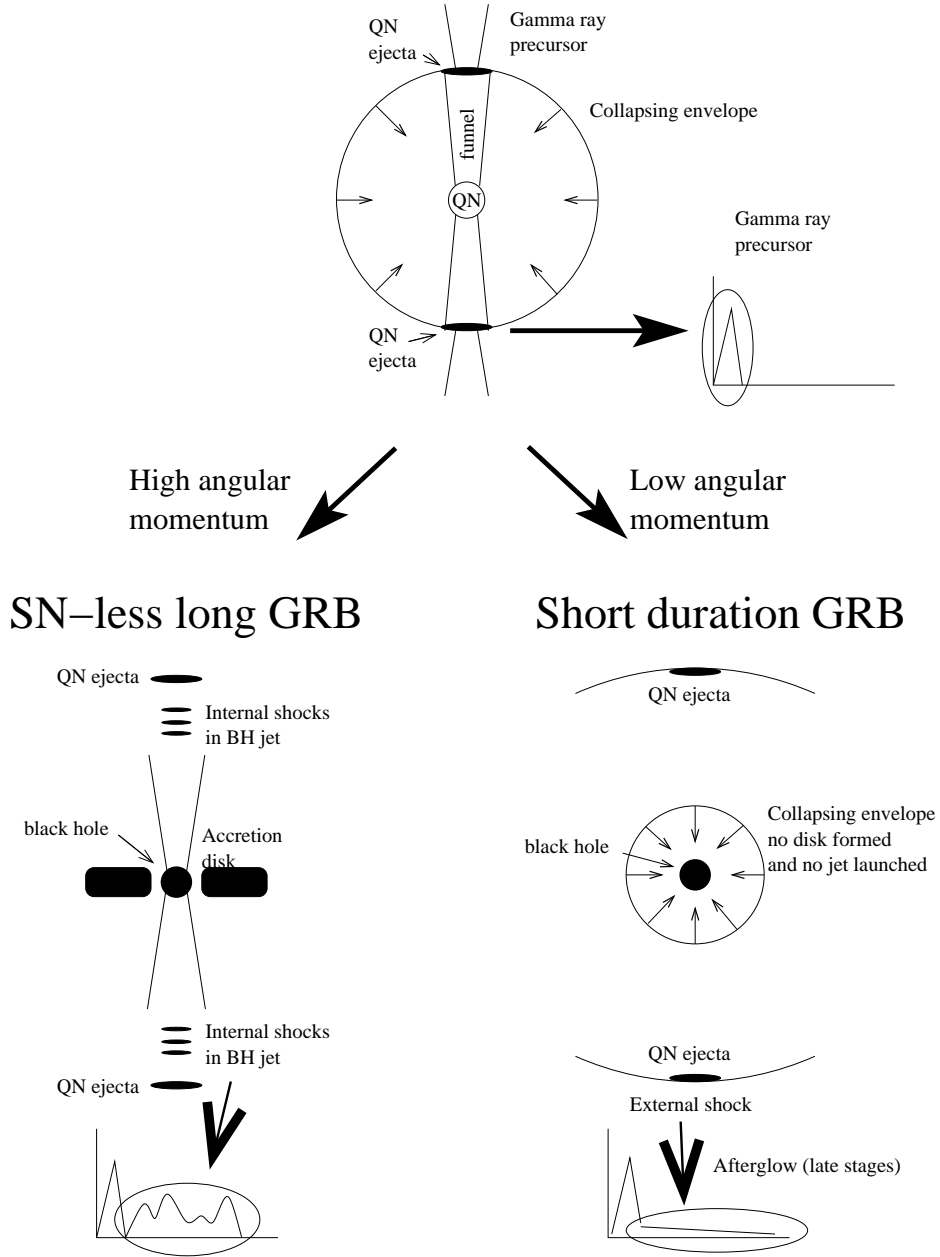


**Fig. 5.** Illustrated here is the case of a QN inside a failed SN (i.e. collapsing envelope). In this case the interaction between the denser envelope material and the QN ejecta would lead to a  $\gamma$ -ray precursor (see §2.1). The two possible outcomes are long and short GRBs with no SN association, depending on the angular momentum of the progenitor. Both cases result in a formation of a black hole with the higher angular momentum case providing an accretion disk and a jet leading to the prompt GRB (see §3.2). The low angular momentum case consists on the  $\gamma$ -ray precursor followed only by an afterglow.

served prompt GRB emissions (e.g. Ryde 2005 and references therein). This is further discussed in §4.7.

### 3.3. Afterglow emission

The shells from the QS jet (following accretion onto the QS) colliding with the cap produce events similar to internal shocks between shells themselves. The cap provides a buffer for the

intermittent shells to be absorbed and subsequently form a heavy, slowly moving “giant” shock (reminiscent of an external shock) that might be of relevance to the afterglow activity. This buffer, of minimum mass  $\theta_f^2 m_{\text{cap}} \sim 10^{-6} M_{\odot} \theta_{f,0.1}^2 m_{\text{cap},-4}$ , will lead to different type of afterglows depending on whether it is relativistic or not.

The slowly moving wall resulting from the merging of the cap and the multiple QS shells should absorb and emit radiation

as it interacts with the surrounding or when it is bombarded by the energetic photons from late internal shocks (e.g. Staff et al. 2006b). Iron emission lines have been detected in the X-ray afterglow of few GRBs (Piro et al. 2000; Butler et al. 2003; Reeves et al. 2002; Watson et al. 2002; Antonelli et al. 2000). This might be indicative of heavy elements in the cap which survive nuclear disintegration due to shocks.

## 4. Discussion

### 4.1. SN-less GRBs in our model

If the supernova fails to explode then the consequences are twofold in our model (see Fig. 5). First, the QN ejecta will be subject to larger densities due to an infalling stellar envelope, which leads to higher shock efficiency  $\xi_s$  and a harder spectrum than if the SN had occurred.

Second, the infalling material will in most cases force the QS to turn into a black hole. Whereas in the SN case the outcome could be a QS or a black hole depending on the disk and QS's initial mass, in the SN-less case the GRB phase is likely due to jet activity from accretion onto a black hole. In our QS model, as opposed to models with just a black hole, the black hole jet will catch up faster with the mixed ejecta/envelope since the QN ejecta will have cleared out the more compact, dense envelope.

### 4.2. Short duration GRBs in our model

The short duration GRBs we first discuss here are necessarily related to star forming regions. A discussion on the second class (i.e. those not associated with star forming regions) in our model will be presented elsewhere. A short duration GRB in our model corresponds to the case of a low-angular momentum progenitor. In this case the infalling progenitor's envelope will not form a disk and will fall entirely onto the star, resulting in a black hole with no surrounding material to accrete (see Figure 5). Simply put, in our model short GRBs are dominated by the precursor phase which will emit in the  $\gamma$ -ray frequency band due to the high envelope densities.

We expect that the funnel's opening angle in this case will be wider than in cases involving disks (from angular momentum arguments). This implies that (i) some short GRBs with no SN association should be found in star forming regions; (ii) they might be less numerous than long ones if low angular momentum progenitors are spars; (iii) they are less luminous and thus only the nearby one will be detectable; (iv) their spectrum should be harder since the QN ejecta will interact with a more dense SN ejecta; (v) X-ray precursors of SN-less GRBs or the early phase of the prompt GRB emission in SN-less GRBs should resemble emission from short GRBs.

### 4.3. Dark GRBs in our model

Dark GRBs are defined as those that are not associated with an optical afterglow (e.g. Jakobsson et al. 2004) or any afterglow emission regardless of the frequency band (e.g. Mészáros et al. 2007). In our model the cap as we have said provides a buffer

for the episodic shocks (from accretion onto the QS) to be absorbed and subsequently form an external shock that could in principle explain the observed afterglows.

One possible explanation using our model is that Dark GRBs would correspond to the situations where the interactions between the cap and the upcoming QS shells are reduced or nonexistent. This would be the case if the envelope is thin in which case there is no cap or buffer, or if the cap is moving at relativistic speeds in which case the heating from the colliding shocks is diminished.

### 4.4. Hypernovae as QNe signature?

Hypernovae are energetic SNe associated with GRBs and are observed in the late afterglows of long GRBs. In our model, outside the funnel where the density is above the critical density, the chunks will dissipate their energy entirely into heat. As shown in Leahy&Ouyed (2008b) this results in a super-luminous supernova reminiscent of a hypernova. Furthermore, conditions in the expanding QN ejecta are favorable for the r-process to take effect (as discussed in details in Jaikumar et al. 2007). Hence, additional heavy elements will be deposited in the expanding envelope as the QN ejecta reaches and mixes with the envelope.

### 4.5. Optical flashes and X-ray precursors

Traditionally, it has been suggested that the optical emission could be produced by the reverse shock emission or could arise from the internal shock emission (e.g. Sari & Piran 1999). Observationally, there appears to be two cases of prompt optical emission:

- For GRB990123 and recently discovered GRB060111b, the optical flashes were uncorrelated with the prompt gamma-ray emission, which suggests that the optical emission and gamma-ray emission should have different origin (e.g. Klotz et al. 2006).
- For GRB041219a, its optical flash was correlated with the gamma-ray emission (Vestrand et al. 2005; Blake et al. 2005), and for GRB050904, a very bright optical flare was temporally coincident with an X-ray flare (Böer et al. 2006; see also Wei 2007), which implies that for these two GRBs there should be a common origin for the optical and high energy emission.

More recently, the near-simultaneous optical and  $\gamma$ -ray emission in GRB 080319B has re-opened this debate. Kumar&Panaitescu (2008) argue for a Synchrotron self Compton (SSC) origin while recent work (Zou, Piran, & Sari 2008) argue for physically separated emission regions (e.g.  $\gamma$ -rays from internal shocks and optical flash from external shock emission).

In our model, the optical emission originates when the chunks are heated during their passage through the thin envelope (see §3.1.1), and X-ray emission when the chunks dissipate further out at the density inversion (high metallicity stars; Petrovic et al. 2006). The optical and X-ray emission are produced at different radii with durations dominated by geometry



as given in Eq.(6) but both composed of short pulses from the  $\sim 10^3$ - $10^7$  chunks. The prompt GRB emission is from internal shocks in the outflow launched during accretion onto the QS (see §3.2), physically separated from the optical emission. The delay of the optical from the QN event can be shorter or longer than the corresponding GRB delay depending on the Lorentz factors and emission distances.

#### 4.6. X-ray flares

X-ray flares are frequently observed in the early X-ray afterglow of GRBs (e.g. Burrows et al. 2005; Chincarini et al. 2007). In Staff, Ouyed, & Bagchi (2007) a possible explanation for these X-ray flares with an accreting quark star as the GRB inner engine is given. A quark star can accrete a maximum of about  $0.1M_\odot$  before collapsing to a black hole. Hence the quark star as GRB inner engine can last for about a thousand seconds. If there is still matter left to accrete once the black hole is formed, a new jet is formed from the accretion onto the black hole (DeVilliers, Staff, & Ouyed 2005). Staff et al. (2007) proposed that the interaction between the jet from the black hole and the jet from the quark star could make internal shocks and thereby produce X-ray flares. Furthermore, when the black hole jet (or more massive parts of the quark star jet) interacts with the external shock, the shock will be reenergized and a “bump” can result. Internal shocks within the black hole jet itself can also occur, giving rise to more flares; see Figure 5 in Staff et al. (2007) for the resulting lightcurves.

The accretion rate onto a black hole is likely very high ( $\dot{M}_{\text{BH}} \sim 0.1 - 1M_\odot \text{ s}^{-1}$ ), meaning the black hole phase will be rather short. The flares created by interactions between the black hole jet and the quark star jet therefore have to occur within about a thousand seconds, whereas the activity caused by interaction between the jets and the external shock can occur later. Flares can occur earlier if the quark star collapses to a black hole sooner than after a thousand seconds.

#### 4.7. The two components

From equation (10) we estimate the expanding cap to becomes optically thin to photons from the internal shocks, at a radius of about  $r_{\text{therm.}} \sim 3 \times 10^{13} \text{ cm } m_{\text{cap},-4}$  at which point the temperature of the thermal component becomes  $T_{\text{eq}} \sim 10 \text{ keV } T_{\text{QS},10} R_{\text{QS},10}^{1/2} / m_{\text{cap},-4}^{1/4}$ . The emission would thus remain thermal for a duration of  $t_{\text{therm.}} \sim r_{\text{therm.}} / (2\Gamma_i^2 c) \sim 10 \text{ s } m_{\text{cap},-4}^{1/2} / \Gamma_{i,10}^2$ . The synchrotron radiation from the subsequent internal shocks will then dominate the spectrum in the later stages,  $r > r_{\text{therm.}}$ , of the prompt GRBs; the QS will continue to accrete until the accretion disk is consumed or the QS turns into a black hole (Ouyed et al. 2005; Staff et al. 2006b). Whether the two-components presumably inherent to some GRBs (Ryde 2005) is an indication of the envelope-shells interaction as described in our model remains to be confirmed. For completeness, however, we should note that accreting quark stars could in principle result, as we have said above, from QNe going off in isolation in which case the standard in-

ternal shocks scenario, involving no intervening envelope, applies (Ouyed et al. 2005).

## 5. Conclusion

In this paper, we explore the case of a QN going off inside a collapsar. We find that the interaction between the iron-rich chunks from the QN ejecta and the collapsar envelope leads to features indicative of those observed in Gamma Ray Bursts. These features include: (i) precursor activity (optical, X-ray,  $\gamma$ -ray), (ii) prompt  $\gamma$ -ray emission, and (iii) afterglow emission. Although the presented model is based on physical arguments, most of these are in reality more complicated and so would require more detailed studies. For example, the launching of the outer layers of the neutron star during the QN is a challenging process to study, and involves energy transfer, core-bounce, generation of a shock wave, including cooling processes, and subsequent ejection. We have assumed simple conditions for the ejecta immediately after the QN such as a single Lorentz factor. A range of Lorentz factors would still result in the outermost shell of the ejected material interacting with the progenitor envelope as we have described here. Shells with lower Lorentz factors would interact later in a similar manner and would lead to more complex interaction with the envelope. Another important aspect of our model that requires further studies is the process of clumping, crystallization, and breakup of the ejecta, which would require better knowledge of the ambient conditions surrounding the ejecta. Despite our simplifying assumptions, we feel that our model captures the basic envelope interaction physics and provides interesting features with possible applications to GRBs.

*Acknowledgements.* This work is supported by an operating grant from the Natural Research Council of Canada (NSERC).

## References

- Antonelli, L.A., et al., 2000, ApJ, 545, L39
- Baym, G., Pethick, C., & Sutherland, P. 1971, ApJ, 170, 299
- Blake, C. H., et al. 2005, Nature, 435, 181
- Böer, M., et al., 2006, ApJ, 638, L71
- Burrows, D. N. et al., 2005, Science, 309, 1833
- Butler, N.R., et al., 2003, ApJ, 597, 1010
- Chincarini, G., et al. 2007, ApJ, 671, 1903
- De Villiers, J.-P., Staff, J., & Ouyed R. 2005 [astro-ph/0502225]
- Granot, J. 2008, astro-ph/0811.1657v2
- Handbook of Chemistry and Physics 2005, B-1 (CRC Press)
- Heger, A. et al. 2003, ApJ, 591, 288
- Jaikumar, P., Meyer, B. S., Otsuki, K., & Ouyed, R. 2007, A&A, 471, 227
- Jakobsson, P. et al. 2004, ApJ, 617, L21
- Keränen, P., & Ouyed, R. 2003, A&A, 407, L51
- Keränen, P., Ouyed, R., & Jaikumar, P. 2005, ApJ, 618, 485
- Klotz, A., Gendre, B., Stratta, G., Atteia, J. L., Böer, M., Malacrino, F., Damerdj, Y., & Behrend, R. 2006, A&A, 451, L39
- Kobayashi, S., Piran, T., & Sari, R. 1997, ApJ, 490, 92

- Kumar, P., & Panaitescu, A. 2008, *MNRAS*, 391, L19
- Leahy, D., & Ouyed, R., 2008a, AIP conference proceedings editors: C.A. Meegan, N. Gehrels, and C. Kouveliotou 6th Huntsville Gamma-Ray Burst Symposium, in press
- Leahy, D., & Ouyed, R. 2008b, *A&A*, *MNRAS*, 387, 1193
- Mészáros, A., Bagoly, Z., Klose, S., Ryde, F., Balázs, S. L. L. G., Horváth, I., & Borgonovo, L. 2005, *Nuovo Cimento C Geophysics Space Physics C*, 28, 311 [astro-ph/0701905]
- Mészáros P. 2006, *Reports on Progress in Physics*, 69, Issue 8, 2259
- Meynet, G., & Maeder, A. 2003, *A&A*, 404, 975
- Nousek, J. A. et al. 2006, *ApJ*, 642, 389
- Ouyed, R., & Leahy, D. 2008, *ApJ*, in press [arXiv:0812.4441]
- Ouyed, R., Dey, J., & Dey, M. 2002, *A&A*, 390, L39
- Ouyed, R., Rapp, R., & Vogt, C. 2005, *ApJ*, 632, 1001
- Petrovic, J., Pols, O., & Langer, N. 2006, *A&A*, 450, 219
- Piro, L., et al., 2000, *Science*, 290, 955
- Reeves, J.N., et al., 2002, *Nature*, 416, 512
- Ryde, F. 2005, *ApJ*, 625, L95
- Sari, R., & Piran, T. 1999, *ApJ*, 520, L641
- Staff, J. E., Ouyed, R., & Jaikumar, P. 2006b, *Astrophys. J. Lett.*, 645, L145
- Staff, J., Ouyed, R., & Bagchi, M. 2007, *ApJ*, 667, 340
- Toma, K., Yamazaki, R., & Nakamura, T. 2005, *ApJ*, 635, 481
- Vestrand et al. 2005, *Nature*, 435, 178
- Vogt, C., Rapp, R., & Ouyed, R. 2004, *Nucl. Phys. A.*, 735, 543
- Watson, D., et al., 2002, *A&A*, 393, L1
- Wei, D. M. 2007, *MNRAS*, 374, 525
- Woosley, S. E., & Bloom, J. S. 2006, *ARAA*, 44, 507
- Zhang, B. 2008, *Astrophysics of Compact Objects*, 968, 9
- Zou, Y. C., Piran, T., & Sari, R. 2008, arXiv:0812.0318